THE EFFECT OF MO MORPHOLOGY ON THE PERFORMANCE OF CU(IN,GA)SE_2 THIN FILMS

Danny C. Fisher[a], Ingrid L. Repins[a], Jeff Schaefer[a], Markus E. Beck[b], Wendi K. Batchelor[a], Matthew Young[c] and Sally Asher[c]

[a] ITN Energy Systems, 8130 Shaffer Pkwy, Littleton, CO 80127

[b] Global Solar Energy, Inc., 5575 South Houghton Road, Tucson, AZ 85747

[c] National Renewable Energy Laboratory, 1617 Cole Blvd., Golden, CO 80401

ABSTRACT

The properties of sputtered and electron-beam evaporated Mo are compared, and the resulting impacts on performance of co-evaporated CIGS devices deposited on each type of back contact are investigated. In past studies, the effect of Mo on Cu(In,Ga)Se_2 device efficiency has been attributed largely to control of sodium diffusion from the glass. To verify this hypothesis, sodium-free Al_2O_3 substrates were utilized. Despite lack of Na in the substrate – Na was provided as NaF on the Mo layer – significant differences in device performance between the two types of Mo were observed. Purely resistive effects are ruled out by sheet resistance measurements, and comparison of current-voltage parameters. Negative contributions due to diffusion of harmful impurities from the substrate can be eliminated based on secondary ion mass spectroscopy results. These findings lead to the deduction of device performance dependency on Mo morphology.

INTRODUCTION

In past studies, the effect of molybdenum (Mo) on Cu(In,Ga)Se_2 (CIGS) device efficiency has been attributed largely to control of sodium diffusion from the glass [1,2]. At the same time, the impact of Mo morphology on CIGS film nucleation [3] has received little consideration. In this study, Mo thin film back contacts were deposited on sodium-free substrates, aluminum oxide (Al_2O_3), using both direct-current magnetron sputtering and electron-beam evaporation. Sodium fluoride (NaF) deposited onto the Mo via electron-beam evaporation provided quantitative amounts of Na for CIGS film growth. Three-stage co-evaporation [4] was employed to deposit a thin film of CIGS onto the Mo/NaF-coated Al_2O_3. Devices showed a substantial performance difference as a function of Mo formation method. The highest recorded efficiency for all cells using DC-sputtered Mo was 10.3%, whereas for evaporated Mo only 6.3% were achieved.

EXPERIMENTAL

Substrates used were 99.5% pure Al_2O_3 wafers of $75 \times 75 \times 0.6$ mm^3 with a surface polished to 510Å average roughness.

Two types of Mo deposition methods were applied; (a) pulsed direct-current magnetron sputtering (hereafter referred to as "sputtered" Mo) and (b) electron-beam evaporation ("e-beamed"). Mo thickness was 7500 Å for both deposition methods. Sputtered Mo was deposited in 2 passes, in an Ar pressure of 7.5 mTorr, at a deposition rate of approximately 32 Å/sec. E-beam depositions were performed at a rate of approximately 2 Å/sec on each substrate. No intentional substrate heating was applied for either type of Mo deposition.

The structural properties of the substrate and resulting metal layers were characterized by scanning electron microscopy (SEM) and X-ray diffraction (XRD). As Na-free Al_2O_3 substrates were employed, 110Å of sodium fluoride (NaF) were deposited onto the Mo films by electron-beam evaporation, following SEM characterization.

Subsequent absorber formation employed three-stage co-evaporation [4] with a maximum temperature of 565°C, resulting in CIGS ranging in thickness from 1.95 to 2.1 µm. Absorber composition was controlled to an atomic ratio Cu/[In+Ga] within 0.85 to 0.95, and 0.32 to 0.36 for atomic ratio Ga/[In+Ga]. Devices were completed via addition of standard layers: 500Å CBD CdS, 500Å pulsed DC-sputtered resistive ZnO, 0.4 µm pulsed DC-sputtered ITO, and e-beam evaporated Ni:Al grids. No anti-reflective coating was applied. Isolation into 1.16 cm^2 active area devices was achieved by mechanical scribe. Each 3" × 3" substrate yielded 30 devices, for a total of 180 in the study. Current-voltage characteristics were evaluated under standard AM1.5 conditions.

CIGS and Mo impurity content were examined by secondary ion mass spectroscopy (SIMS) prior to CdS deposition. SIMS system conditions were a Cs^+ primary beam at ±4.5 kV secondary accelerating voltage and a primary current of ~200 nA. The area analyzed was ~20 µm in diameter for the negative atomic and positive molecular ions, and ~60 µm for the positive atomic ions. Positive atomic ion data was used for Al analysis, while negative atomic ion data was used to trace O through the sample.

RESULTS AND DISCUSSION

CIGS device performance, Mo morphology, Mo sheet resistance, and possible impurity diffusion were evaluated as a function of Mo deposition method. Sputtered and e-beamed Mo films show vastly different surface morphology when characterized by SEM. The sputtered films exhibit porous and fibrous grains, as illustrated in Figure 1, while the e-beamed films yield a dense, tightly packed, small-grain microstructure (Figure 2). For optimal CIGS growth on soda lime glass, it has been reported that the most desirable Mo films display a fibrous morphology more like that of the sputtered film [1,2]. The difference in Mo grain size was confirmed via XRD, as was a consistent (110) orientation for both types of Mo.

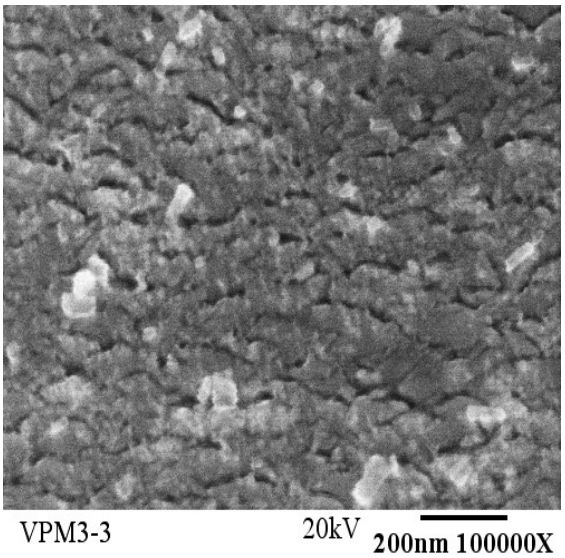

Figure 1. SEM plan-view of a Mo film deposited onto Al_2O_3 using dc-magnetron sputtering.

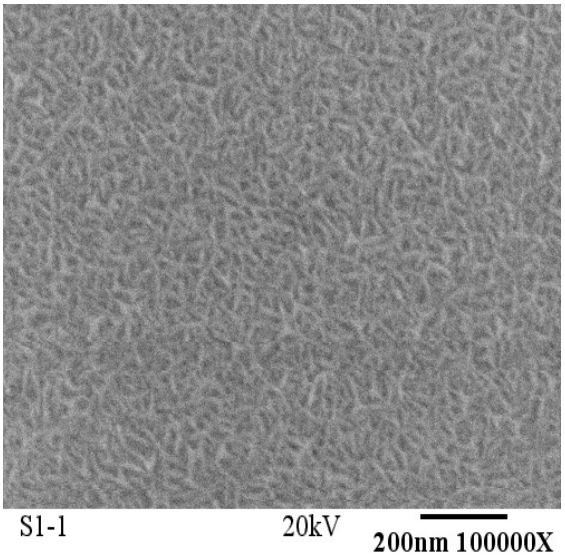

Figure 2. SEM surface image of electron-beam evaporated Mo on Al_2O_3.

Table 1 summarizes the average device performance data for each substrate; maximum values are listed in parentheses. Average I-V parameters exclude devices with fill factor values of less than 30%, assigning the losses to localized defects. An absolute efficiency difference of almost 6% exists between average values (4% for maximum values) of the devices on sputtered versus e-beamed Mo. Light current-voltage curves for the best devices representative of each Mo deposition method are graphed in Figure 3.

Table 1. Comparison of average and maximum CIGS device performance results as a function of Mo deposition method.

Substrate	Mo Dep. Method	Efficiency (%)	Voc (Volts)	Jsc (mA/cm2)	FF (%)
1	e-beamed	3.88 (4.94)	0.38 (0.40)	30.95 (33.40)	0.33 (0.40)
2	e-beamed	4.00 (6.29)	0.38 (0.42)	30.09 (32.80)	0.35 (0.49)
3	e-beamed	4.84 (6.76)	0.42 (0.46)	30.09 (31.13)	0.38 (0.47)
4	rf-sputtered	9.91 (10.3)	0.51 (0.52)	33.43 (34.10)	0.59 (0.62)
5	rf-sputtered	9.5 (10.2)	0.48 (0.51)	34.18 (34.90)	0.58 (0.61)
6	rf-sputtered	7.61 (8.98)	0.51 (0.52)	28.11 (29.81)	0.53 (0.58)

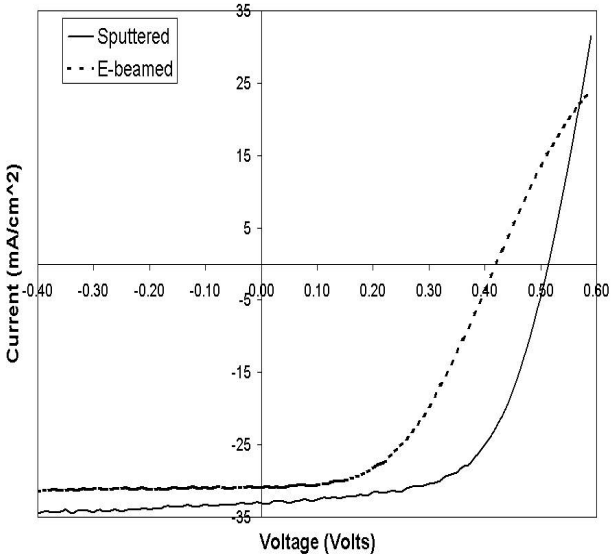

Figure 3. Comparison of light I-V curves for the best devices with sputtered and e-beamed Mo on Al_2O_3 substrates.

In order to attribute the large efficiency differences (see Table 1) to Mo morphology, sheet resistance effects need to be ruled out. The lateral sheet resistance values of the Mo films were measured using a four-point probe applying a current of 100 mA. For the sputtered Mo, sheet resistance averaged 0.66 Ω/square, while for the e-beamed Mo, average sheet resistance was 5.7 Ω/square. Although the e-beamed Mo has a sheet resistance almost one order of magnitude higher than that

of the sputtered film, the associated calculated fractional power loss, due to lateral current flow, is actually relatively small. The calculated efficiency loss [5] for depositing a 10% device on 5.7 Ω/square Mo is only 0.35%. This implies that resistive losses in the Mo alone should yield devices at the 9.65% efficiency level rather than the observed 6% for e-beam evaporated Mo. Thus, lateral resistance losses in the Mo are not large enough to account for the effects described in Table 1. Furthermore, the I-V curves in Figure 3 illustrate significant differences in open-circuit voltage and current collection, implying sizable contributions other than resistive losses.

The above analysis of resistance considers lateral current flow only, while contact resistance between the CIGS and Mo is not addressed. The latter has been reported to be defined by the degree of $MoSe_2$ formation [6]. The contact of CIGS to Mo is reported as rectifying, while becoming ohmic with the formation of $MoSe_2$. Thus, the structure of the e-beamed Mo – devices on these substrates exhibit moderate fourth quadrant roll-over and reduced slope near V_{oc} – may hinder $MoSe_2$ formation as compared to increased Mo selenization of the sputtered Mo. Unfortunately, due to peak overlap of $MoSe_2$ and Al_2O_3 reflections X-ray diffraction does not allow quantitative analysis to investigate potential differences in $MoSe_2$ formation on the two Mo types during CIGS growth.

In order to validate the hypothesis of Mo morphology being the underlying cause of the observed device performance differences, possible effects of aluminum and oxygen (from the substrate) diffusing through the Mo must also be eliminated as possible causes. Al_2O_3 substrates are not expected to be strong diffusers of harmful impurities as the ceramic material can be considered to be chemically inert, and high-efficiency devices have been deposited onto Al_2O_3 without employing diffusion barriers [7]. SIMS profiles were acquired to insure that out-diffusion of Al or O from the substrate through the Mo layer is not responsible for the device performance differences.

The oxygen content throughout the Mo and CIGS layers is plotted in Figure 4 for samples representative of CIGS on sputtered as well as e-beamed Mo – in total 6 CIGS-coated specimens were analyzed. The vertical line roughly indicates the position of the Mo/CIGS interface. In a similar fashion, Figure 5 shows the Al content in the CIGS and Mo films. Both, the oxygen and aluminum profiles for e-beamed and sputtered Mo are very similar. In the case of the Al profile, an upward spike is evident for both deposition methods at the CIGS/Mo interface. It is not apparent whether this signal change reflects a true increase in the Al content or is a result of SIMS matrix effects at the interface. However, the Al level between different samples in a given layer can be compared – the number of counts from Al in the CIGS for the sputtered sample should have the same relationship to concentration in the e-beamed sample. This holds true for the Mo layers between the two sets, although there might be some slight differences due to the different morphologies and oxygen contents – the high levels of O in the Mo layer likely indicate MoO_x. The additional spikes in the sputtered Mo are a consequence of the bi-layer nature for these back contacts.

Based on these results, it can be concluded that diffusion of Al or O were not responsible for the performance differences between devices on sputtered and e-beamed Mo.

Post CIGS deposition X-ray diffraction analysis did not reveal differences in preferred orientation (220/204), but slightly reduced grain size for the absorbers deposited on the e-beamed Mo back contacts (Figure 6). These differences are confirmed via x-section SEM imaging (Figure 7). Hence, the different surface morphologies of the two Mo back contact types can be directly linked to crystallographic differences of the absorbers independent of Na availability, in turn impacting device performance.

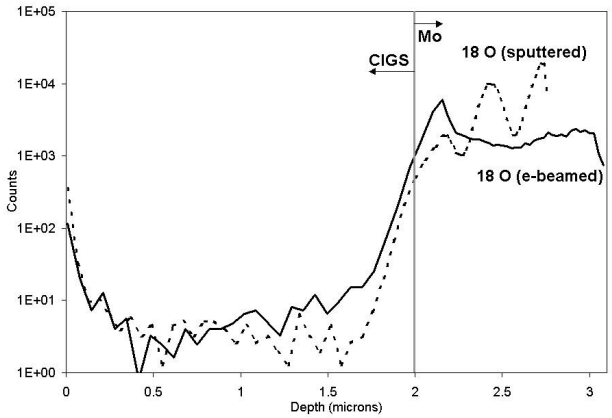

Figure 4. Oxygen profile (SIMS) in CIGS and Mo deposited onto Al_2O_3 substrates.

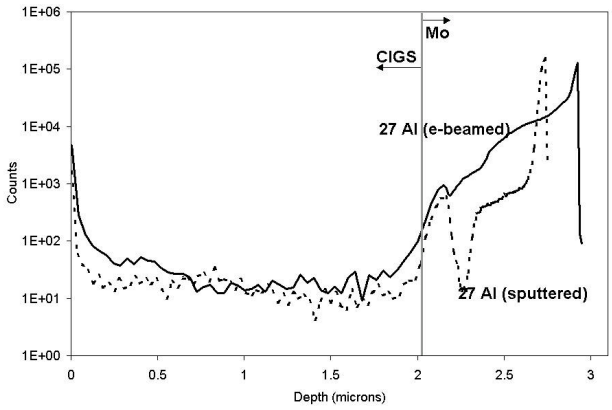

Figure 5. SIMS data plotting Al content in CIGS and Mo deposited onto Al_2O_3 substrates.

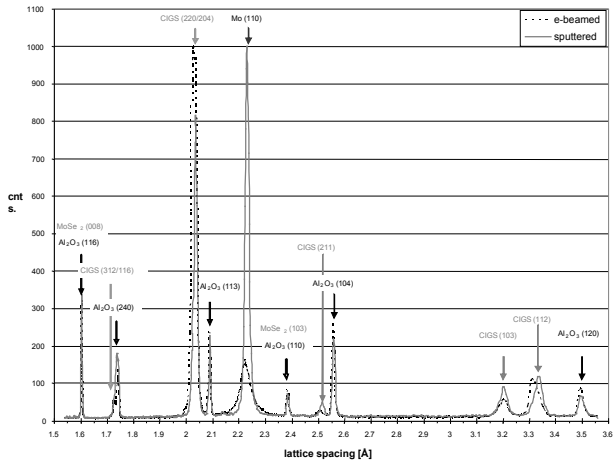

Figure 6. X-ray diffraction patterns of CIGS grown on e-beam evaporated and dc sputtered Mo back contacts on Al_2O_3 substrates.

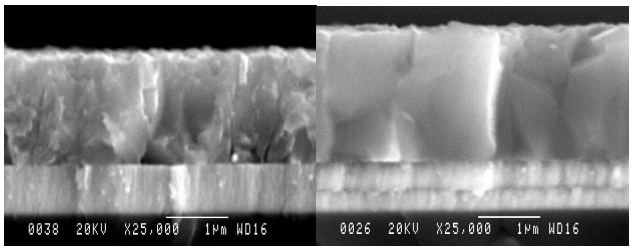

Figure 7. X-section micrographs for CIGS grown on e-beam evaporated (left) and dc sputtered (right) Mo back contacts on Al_2O_3 substrates.

CONCLUSION

Studying the impacts of Mo deposition methods on CIGS-based devices led to the conclusion that the morphology of the Mo layer has a significant effect on resulting device characteristics. The role of Mo morphology has been isolated from substrate related Na effects via use of Al_2O_3 as the substrate and quantitative Na introduction via NaF precursors deposited onto the Mo films. Porous and fibrous Mo grains allow for higher efficiency devices when compared to a dense, tightly packed, small-grain Mo microstructure. The crystallographic differences of the Mo layer directly impact CIGS nucleation and grain growth independent from Na availability. In the present study the different back contact morphologies were achieved by selecting adequate deposition parameters for dc sputtering and e-beam evaporation of Mo. It should be noted that the different Mo morphologies are not a result of the deposition method as such. Resistive differences between the two types of Mo were ruled out as the underlying cause for the performance differences, as were differences in aluminum and oxygen diffusion through the Mo and structural CIGS differences.

ACKNOWLEDGEMENTS

This research was funded by Unisource Energy Corporation and the National Renewable Energy Laboratory through subcontract #NDJ-2-30630-14 to Global Solar Energy. The authors are grateful to Rosine Ribelin and Paul DuPont for Mo depositions (ITN Energy Systems), as well as Bobby To from NREL for SEM images.

REFERENCES

[1] Hamda A. Al-Thani, Falah S. Hasoon, Matt Young, Sally Asher, Jeff L. Alleman, Mowafak M. Al-Jassim, Don L. Williamson, "The Effect of Mo Back Contact on Na Out-Diffusion and Device Performance of Mo/Cu(In,Ga)Se_2/CdS/ZnO Solar Cells", *Twenty-Ninth IEEE Photovoltaic Specialist Conference*, 2002, pp. 720-723.

[2] J. L. Alleman, H. Al-Thani, R. Noufi, H. Moutinho, M. M. Al-Jassim, F. Hasoon, "Dependence of the Characteristics of Mo Films on Sputter Conditions", *NCPV Program Review Meeting*, 2000, pp. 239-240.

[3] M.A. Contreras, B. Egaas, D. King, A. Swartzlander, T. Dullweber, "Texture manipulation of CuInSe2 thin films", *Thin Solid Films 361-362*, 2000, pp. 167-171.

[4] Andrew M. Gabor, John R. Tuttle, David S. Albin, Miguel A. Contreras, "High-efficiency $CuIn_xGa_{1-x}Se_2$ solar cells made from $(In_x,Ga_{1-x})_2Se_3$ precursor films", *American Institute of Physics*, 1994, pp. 198-200.

[5] See, for example, M.A. Green, *Solar Cells*, Prentice-Hall, (1982), pg. 146 ff.

[6] N. Kohara, S. Nishiwaki, Y. Hashimoto, T. Negami, T. Wada, "Electrical properties of the Cu(In,Ga)Se_2/Mo Se_2/Mo structure", *Solar Energy Materials & Solar Cells 67*, 2001, pp. 209-215.

[7] Granata et al, AIP 394, (1996), pg. 621 ff.